International Journal of Current Engineering and Technology
E-ISSN 2277 – 4106, P-ISSN 2347 – 5161

Available at http://inpressco.com/category/ijcet

Research Article

Design and Optimization of Printed Spiral Coils used in Wireless Power Transmission Systems for Powering 10 mm² Receiver Size at 13.56 MHz Operating Frequency

Ahmed S. Ezzulddin and Ahmed A. Ibraheem*

Department of Electrical Engineering, University of Technology, Baghdad- Iraq

Received 14 Aug 2017, Accepted 01 Oct 2017, Available online 08 Oct 2017, **Vol.7, No.5 (Sept/Oct 2017)**

Abstract

Due to size limitations and limited battery life, many implant biomedical devices need to be powered inductively. This paper introduces a small size and efficient spiral square coils at 13.56 MHz to be used for bio-implantable devices. We applied our design methodology with theoretical closed-form equations using MATLAB to optimize the wireless link of a 10 mm² implantable device example with 10 mm relative distance. The results showed that optimized coil pairs achieved 73.46% efficiency at face to face relative distance of 10 mm in the air. All results are validated with the simulation using an electromagnetic field solver HFSS 14.1.

Keywords: *Wireless power transfer, inductive coupling, implant biomedical devices, printed spiral coil.*

1. Introduction

Wireless power transfer (WPT) via inductively coupled coils has triggered a great interest of research, related to its wide collection of applications, such as wireless power transfer to desktop peripheral (P. Meyer, P. Germano, M. Markovic, & Y. Perriard, 2011), contactless battery charger (E. Waffenschmidt, 2011, H. Marques & B. Borges, 2011), and implanted biomedical devices (U. Jow & M. Ghovanloo, 2007, U. Jow & M. Ghovanloo, 2009, W. Wu and Q. Fang, 2011, S. Mutashar, M. A. Hannan, S. A. Samad, & A. Hussain, 2014 , S. Stocklin, T. Volk, A. Yousaf, J. Albesa & L. Reindl, 2015, S. Mehri, A. C. Ammari, J. Ben, H. Slama, & H. Rmili , 2016, C. Yang, C. Chang, S. Lee, S. Chang, & L. Chiou , 2017).

The use of a wireless inductive link to transfer power and data to implanted microsystems devices is raising. The main design interest in the implantable devices field is to reduce the patient discomfort and hazard of infection. Usually, implanted devices are obtaining power using implanted batteries, cause chemical burns and risks. Because of the chemical side effect of the implanted and its limited lifetime, researchers have developed an appropriate substitute method for powering implanted devices using inductively coupled power link. It believed that the inductive link approach is the most favorable technique for implanted devices. Its advantages ensure continuous availability of enough levels of power to the implanted devices. In addition, WPT can be used for a long time and within the patient's activities.

Implanted biomedical devices designed with size as small as possible to be implanted based on human biological tissues functional depth, which is typically less than 10 mm. In general, implanted microsystem stimulators need depth (1–4) mm, for cochlear implant depth is (3–6) mm and retinal implant it is 5 mm, respectively (G. M. Clark, 2003, M. S. Humayun et al., 2003).

The WPT inductive coupling link consists of transmitter and receiver coils, acting as two RLC circuits. To obtain maximum power transmission efficiency, both coils circuits are tuned at the same resonant frequency f. The transmitter side uses a serial-tuned to provide the low impedance to the driven side and the receiver side uses parallel with better drive non-linear rectifier loads (L. Chen, S. Liu, Y. C. Zhou, & T. J. Cui, 2013).

The coupling distance between the transmitter and receiver coils is to be less than the wavelength within the near-field, which depends on the coils dimensions. Hence, the coils dimensions have a direct impact on the distance and a coupling link, which consists of two same sized or differing coils, oriented face to face. The receiver coil placed within the human body should be smallest possible size whereas; the transmitter coil can be set with flexibility in the design in term of size since it placed outside the body.

The biggest power loss typically happens in the transmitter coil parasitic resistance R_{s1} followed by R_{s2} and the power load condition within R_L on the

*Corresponding author's ORCID ID: 0000-0003-1835-4862

receiver side. The latter deemed to be more influential because it is surrounded by the tissue (G. Lazzi, 2005). There is also power loss within the external source, which typically represents an efficient class-E power amplifier. If the operation frequency is chosen below 20 MHz, the power loss within the surrounding tissue can be ignored (S. Stocklin, T. Volk, A. Yousaf, J. Albesa & L. Reindl , 2015, P. Vaillancourt, A. Djemouai, J. F. Harvey & M. Sawan, 1997). We choose 13.56 MHz ISM band which compatible with RFID standards (K. Finkenzeller, 2010). The overall power transmission efficiency is often dominated by efficiency link η_{link} between transmitter and receiver which we will focus during the rest of this paper.

The power transfer efficiency is dependent on the coupling coefficient (k) between the transmitter and receiver coils, and the quality factors of the coils. So, to achieve high power transmission efficiency, these parameters of the link should be as high as possible.

Recently, using a printed spiral coil (PSC) in inductive coupling links has got a considerably of attention. In comparison with wire-wound coils, this type of coils has an advantage from a planar structure which makes them more suitable for implanted systems located underneath the skin or within the epidural space. Furthermore, PSCs can be easily manufactured by standard fabrication technologies.

In this paper, optimal printed spiral coil pair used in wireless power transfer system for implanted bio-medical devices is proposed, with external coil dimension d_{o1}= 32 mm and d_{i1}= 6 mm and implant coil dimension d_{o2}= 10 mm and d_{i2}= 5 mm by printed on FR4 substrate to achieve coupling distance 10 mm using industrial, scientific and medical (ISM) band operating frequency 13.56 MHz.

2. Theoretical Model of Printed Spiral Coil (PSC)

Printed spiral coil (PSC) with its equivalent lumped elements are shown in Fig. 1 consist of inductance (L), series parasitic resistance (R_s), and parallel parasitic capacitance (C_p), these parameters affected by various geometries, such as inner diameter (d_i), outer diameter (d_o), number of turns (n), line width (w) and track separation (s) of copper line. The following physical expressions illustrate the relationship between the PSC geometries and its equivalent circuit parameters values.

A. Self-inductance

Numerous closed-form equations propositioned to estimate the inductance in PSC. The inductance of square PSC is shown in Fig. 1(a) can be calculated from (1) given in (S. S. Mohan, M. del Mar Hershenson, S. P. Boyd, & T. H. Lee, 1999). In this paper, all PSCs design are square-shaped with rounded corners to eliminate sharp edges

$$L = \frac{1.27\,\mu n^2 d_{avg}}{2}\left[\ln\left(\frac{2.07}{\varphi}\right) + 0.18\varphi + 0.13\varphi^2\right] \quad (1)$$

where $\mu = \mu_o\mu_r$ is the relative permeability of space and the conductor, n is the number of turns, $d_{avg} = (d_i+d_o)/2$ is the average diameter of the coil, and $\varphi = (d_o-d_i)/(d_o+d_i)$ is the fill factor.

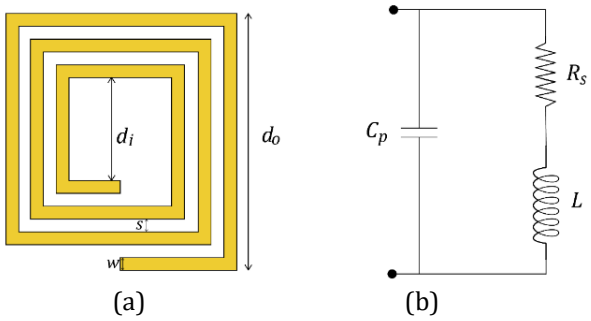

Fig. 1: (a) Geometrical parameters of a square shaped PSC. (b) The equivalent circuit of PSC

B. Series-resistance

To find the parasitic DC resistance for the PSC, we need to know the total length of the conductive line l_c, conductive material resistivity ρ_c, and it's thickness t_c

$$l_c = 4nd_{avg} - n(0.5w + s) \quad (2)$$

$$R_{dc} = \rho_c \frac{l_c}{w.t_c} \quad (3)$$

where w is line width and s track separation. At high frequencies, the ac resistance after taking into account the skin effect can be approximated as (U. Jow & M. Ghovanloo, 2007).

$$R_s = R_{dc}\cdot\frac{t_c}{\delta(1-e^{-t_c/\delta})} \quad (4)$$

$$\delta = \sqrt{\frac{\rho_c}{\pi\mu f}} \quad (5)$$

where δ is skin depth.

B. Parallel-parasitic capacitance

A parallel conductor lines between sidewalls of spiral conductor forms parasitic capacitor with the air and FR4 substrate dielectric Fig. 2. This parasitic capacitor can be estimated after dividing C_p into C_{pc} and C_{ps} (U. Jow & M. Ghovanloo, 2007).

$$C_p = C_{pc} + C_{ps} = \frac{(\alpha\epsilon_r+\beta\epsilon_{FR4})\epsilon_o t_s l_g}{s} \quad (6)$$

where ϵ_r and ϵ_{FR4} are relative dielectric constants of the air and FR4 material, respectively, (α, β) = (0.9, 0.1), and t_s is the thickness of the substrate. The length of the gap (l_g) can be calculated from (7).

$$l_g = 4d_{avg}(n-1) \quad (7)$$

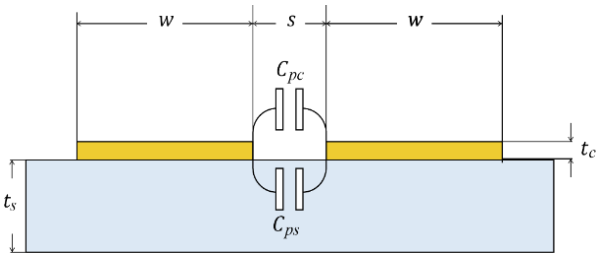

Fig. 2: The cross section of parallel conductor lines showing the parasitic capacitor within the air and substrate

C. PSC quality factor

The quality factor is defined as $Q = \frac{\mathrm{Im}(Z)}{\mathrm{Re}(Z)}$ where Z is the overall impedance of the model. Since R_s is in series with L and C_p is in parallel with both (see Fig1. (b)) (U. Jow & M. Ghovanloo, 2007). This result in (8) and (9)

$$Z = \frac{R_s + j\omega L}{1-\omega^2 L C_p + j\omega R_s C_p} \quad (8)$$

$$Q = \frac{\omega L - \omega(R_s^2 + \omega^2 L^2)C_p}{R_s}. \quad (9)$$

Quality factor can be approached as $Q = \omega L/R_s$ intended for small C_p or low frequency.

D. Mutual Inductance and Power Transfer Efficiency

Printed spiral coils have different forms, line width, line separation, and turn numbers. These are the essential geometric parameters to determine M between the PSCs. The outer radii are r_{o1} and r_{o2}, and the number of turns n_1 and n_2. The line widths are defined as $w_1$and w_2 and s_1 and s_2 are track separations for the primary and secondary PSCs, respectively. To determine the M between the PSCs, it is a necessity to find all of the possible combinations of M by assuming each turn as a rectangular line. And finally, total M can be determined by adding all these combinations of M. For different axial distance, the equation can be expressed as (S. Raju, R. Wu, M. Chan, and C. P. Yue, 2014).

$$M = \left(\frac{4}{\pi}\right)^{\nu} \sum_{i=1}^{i=n1} \sum_{j=1}^{j=n2} M_{ij} \quad (10)$$

and

$$M_{ij} = \frac{\mu_o \pi a_i^2 b_j^2}{2(a_i^2 + b_j^2 + {d_r}^2)^{3/2}} \left(1 + \frac{15}{32}\gamma_{ij}^2 + \frac{315}{1024}\gamma_{ij}^4\right) \quad (11)$$

where $a_i = r_{o1} - (n_i - 1)(w_1 + s_1) - w_1/2$, $b_i = r_{o2} - (n_j - 1)(w_2 + s_2) - w_2/2$,
$\gamma_{ij} = 2a_i b_j/(a_i^2 + b_j^2 + {d_r}^2)$, $\nu = 1 + r_{i2}/r_{i1}$, and d_r is relative distance between coils.

Fig. 3 is clearly elucidated an equivalent circuit diagram of wireless power transfer WPT link. L_1 and L_2 are the inductance of the primary and secondary PSCs, respectively. L_1 is typically driven by class E amplifier which has need of only a single transistor switch and has the benefit of high efficiency. C_p and R_s are the parasitic capacitance and resistance of PSCs, respectively. C_1 and C_2 are tuning capacitors added to PSCs to make the transmitter and receiver resonate on the same frequency.

Using M, L_1 and L_2, the coupling coefficient of the two coil which is the key factor in power transmission efficiency and can be found from (12).

$$k = \frac{M}{\sqrt{L_1 L_2}} \quad (12)$$

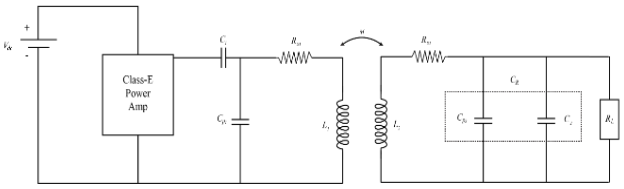

Fig. 3: Equivalent circuit diagram of WPT link

In practice, the secondary coil loaded by some electrical loads such as voltage regulator and rectifier. These loads are epitomized by load resistance R_L. At different loading condition, Power transfer efficiency link can be calculated after introduce loaded quality factor Q_L as (S. Raju, C. C. Parawoto, M. Chan, & C. P. Yue, 2015)

$$Q_L = 2\pi f C_R R_L \quad (13)$$

$$\eta_{\mathrm{link}} = \frac{k^2 Q_1 Q_2^2}{(Q_L + Q_2)\left(\frac{Q_2}{Q_L} + k^2 Q_1 Q_2 + 1\right)} \quad (14)$$

Maximum power transfer efficiency can be determined as

$$\eta_{\mathrm{max}} = \frac{k^2 Q_1 Q_2}{\left(1 + \sqrt{1 + k^2 Q_1 Q_2}\right)^2} \quad (15)$$

In PSCs, most above-mentioned parameters are associated. For instance, increasing n for each coil without changing d_o can increase L and M. As well, it may decrease Q by increasing R_s as a result of increased l_c and reduced w. So, there is optimal PSCs geometry that would maximize efficiency. Other parameters, like eddy current and substrate loss, also be part of the cause, which are not involved in detail due to their small effects.

3. Optimization of Printed Spiral Coils

A design procedure has been represented in this part which starts with a set of initial values and design constraints imposed by the application and fabrication process of the PSC and ends with the optimal PSC pair geometries that maximize efficiency. MATLAB simulation has been used for fine tuning the values based on a theoretical calculation by sweeping many parameters involved in (1)-(15).

Biomedical application place a lower limit on the distance between two coils and upper limit on the size of the coil receiver (d_{o2}), which is typically implanted in the body. We have designated the size of the implanted to be 10×10 mm^2. The coupling distance between the PSCs (d_r) is considered 10 mm. The choice of the optimum operation frequency depends on efficiency, size, and absorption. If the operating frequency of power carrier is below 20 MHz, the power loss within a human tissue can be low. A 13.56 MHz ISM band which compatible with RFID standards has been chosen. Table I shows the initial values and design constraints decreed by the application and fabrication process technology.

The best select for d_{o1} would be 32 mm with smallest possible d_{i1} as illustrated in Fig. 4. Again by fixing d_{o1} at 32 mm, Fig. 5 show the optimal d_{i2} between 6 mm to 7 mm. Our chosen value d_{i1}= 6 mm, so that the magnetic field is not dispensed, and d_{i2}= 5 mm to allow us to achieve a higher inductance and higher quality factor.

Like many previous designers (S. Stocklin, T. Volk, A. Yousaf, J. Albesa & L. Reindl, 2015, R. R. Harrison, 2007), we use a class-E amplifier to drive the coil, suitable to be used in biomedical implantable devices which is usually have a small load resistor due to inductive powering (S. M. Abbas, M. A. Hannan, & A. S. Salina, 2012). This will restrict n_1 according to transmitted coil inductance L_1 captured by (1). To find the value of n_2 Fig. 6 illustrate the changing of n_2 with the efficiency at 500Ω load, The maximum point gives the optimum number of receiver coil turns n_2 that maximize efficiency. The final results of the optimized design example after recalculated the parameters to obtain realistic values shown in Table II. Fig. 7 summarizes the PSCs design procedure steps in a flowchart.

Table 1: Design constraints and initial values imposed by application and fabrication technology

Parameters		Symbol	Design Value
Design constrains	Receiver coil outer diameter	d_{o2}	10 mm
	Distance between coils	d_r	10 mm
	Operating frequency	f	13.56 MHz
	Secondary load resistance	R_L	500 Ω
	Minimum conductor spacing	s_{min}	0.15 mm
	Conductor thickness	t_c	0.07 mm
	Resistivity of material	ρ	16.8 nΩm
	Substrate thickness	t_s	1 mm
	Substrate dielectric constant	ϵ_{rFR4}	4.4
Initial values	Receiver inner diameter	d_{i2}	5 mm
	Transmitter conductor spacing	s_1	0.25 mm
	Receiver conductor spacing	s_2	0.15 mm
	Transmitter and receiver conductor width	w_1, w_2	0.15 mm

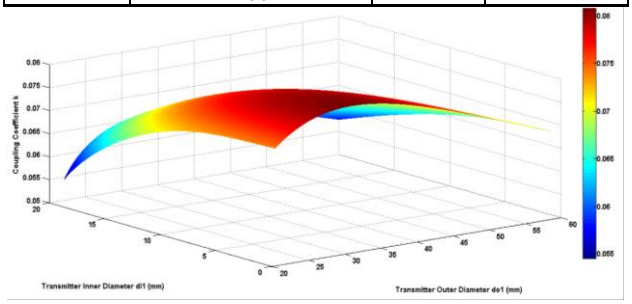

Fig. 4: Optimizing the d_{o1} and d_{i1} of PSCs while d_{o2} and d_{i2} are 10 mm and 5 mm respectively at d_r =10 mm, f = 13.56 MHz.

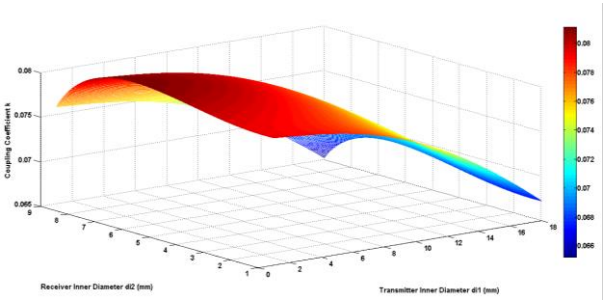

Fig. 5: Optimizing the d_{i1} and d_{i2} of PSCs while d_{o1} and d_{o2} are 32 mm and 10 mm respectively at d_r = 10mm, f = 13.56 MHz

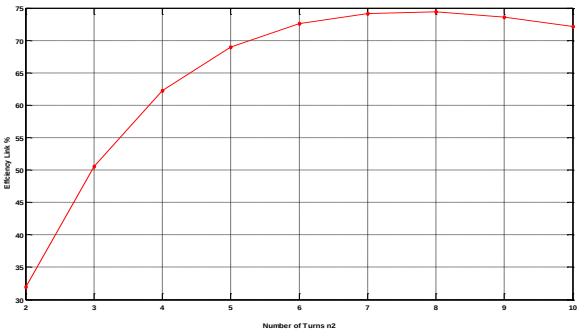

Fig. 6: Optimizing the number of turns of the secondary PSC at 500Ω load

Table 2: Optimized PSCs geometries from theoretical design procedure results

Parameters	TX	RX
d_o (mm)	32	10
d_i (mm)	6.1	5
n (turns)	16	8
w (mm)	0.55	0.16
s (mm)	0.25	0.15

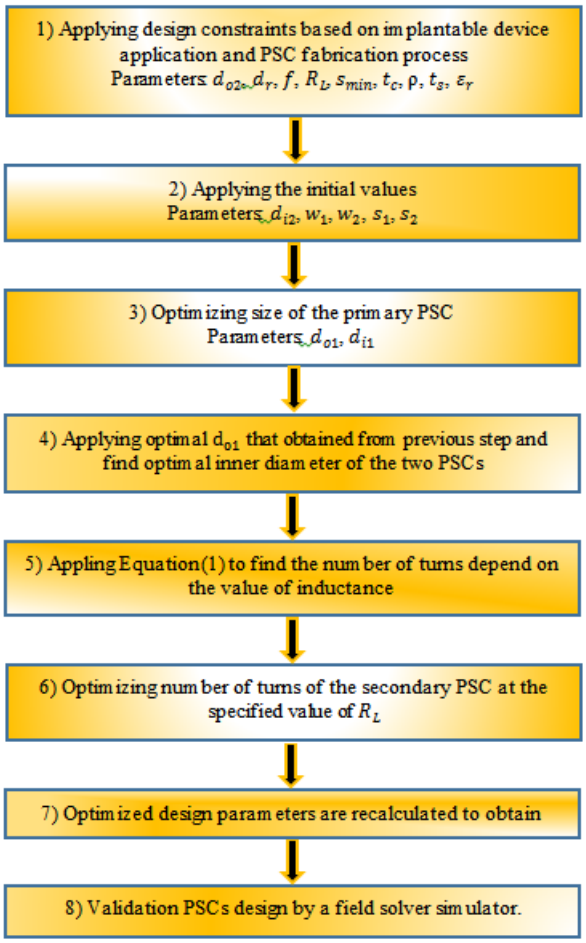

Fig. 7: Optimal PSCs design procedure

4. PSC Simulation and Results

To verify the model, Fig. 8 shows the model of PSCs constructed in HFSS 14.1 on a distance in the air to find the electromagnetic efficiency. The inductance, resistance, parasitic capacitance, quality factor and coupling coefficient can be calculated from Z-parameter by using (18)-(22) (W. Wu & Q. Fang, 2011, S. Mehri, A. C. Ammari, J. Ben, H. Slama, & H. Rmili , 2016, Z. Yang, W. Liu, & E. Basham, 2007).

$$L_1 = \frac{\mathrm{Im}(Z_{11})}{2\pi f}, L_2 = \frac{\mathrm{Im}(Z_{22})}{2\pi f} \quad (16)$$

$$Q_1 = \frac{\mathrm{Im}(Z_{11})}{\mathrm{Re}(Z_{11})}, Q_2 = \frac{\mathrm{Im}(Z_{22})}{\mathrm{Re}(Z_{22})} \quad (17)$$

$$C_{p1} = \frac{1}{4\pi^2 SRF1^2 L_1}, C_{p2} = \frac{1}{4\pi^2 SRF2^2 L_2} \quad (18)$$

$$R_{s1} = \mathrm{Re}(Z_{11})\left(1 - 4\pi^2 f^2 L_1 C_{p1}\right)^2, \quad R_{s2} = \mathrm{Re}(Z_{22})(1 - 4\pi^2 f^2 L_2 C_{p2})^2 \quad (19)$$

$$k = \sqrt{\frac{\mathrm{Im}(Z_{12})\mathrm{Im}(Z_{21})}{\mathrm{Im}(Z_{11})\mathrm{Im}(Z_{22})}} \quad (20)$$

To compute maximum power transmission efficiency, equation (15) was chosen. The simulations of the WPT link were achieved at different transmission distances. In all these case, the inductance and resistance almost remain unchanged, but the mutual coupling was affected directly by this change. This effect was captured by (11). Maximum efficiency of WPT link at different operating frequencies shown in Fig. 9. The simulation tests were done for 10 mm transmission distance to determine the maximum efficiency of the power transmission in the entire range of operating frequencies. The result can clearly identify the power transmission efficiency value at desired operation frequency also illustrated the optimal operating frequency at which the power transmission efficiency reaches its peak value at 25 MHz.

Fig. 10 compares the maximum power transmission efficiency (η_{max}) at different relative distances whereas the operation frequency fixed at 13.56 MHz. The results show that the calculated and simulated values are in agreement. In the next step of simulation were accomplished to capture the effect of load resistance on the power transmission efficiency (η_{link}). The load resistance was varied whereas the transmission distances and operation frequency was kept at 10 mm and at 13.56 MHz, respectively. Fig. 11 verifies that η_{link} reach toward η_{max} at an optimal load resistance of 500 Ω. Again the proposed model has given the simulation results in an agreeable manner. Employing this model, designers can realize the optimal operating condition and design the best efficient WPT system. The final geometries and parameters results of the applied WPT link are defined in Table III.

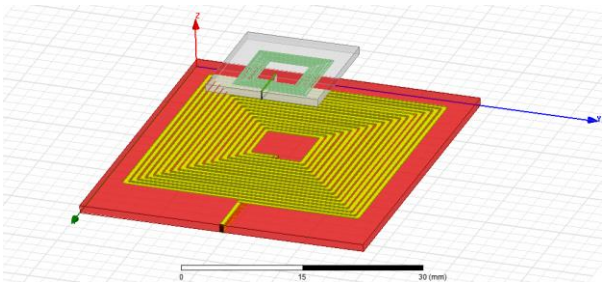

Fig. 8: 3D PSC model constructed in the electromagnetic field solver

HFSS 14.1 simulator

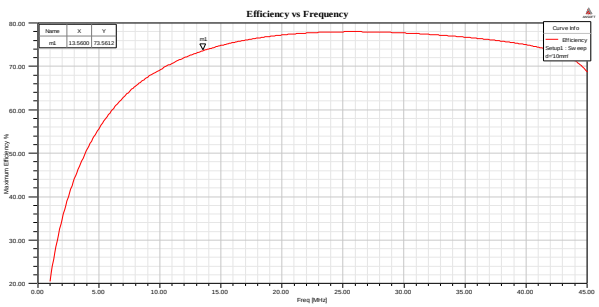

Fig. 9: Maximum power transmission efficiency at 10 mm distance for a different operating frequency

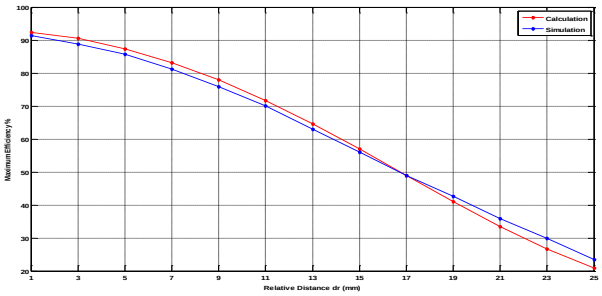

Fig. 10: Maximum power efficiency at different transmission distance at 13.56 MHz

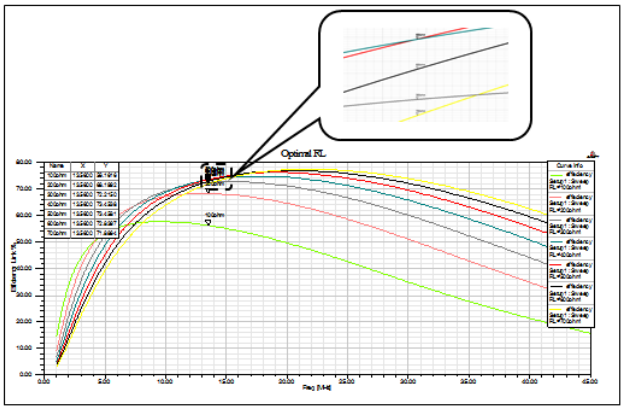

Fig. 11: Efficiency of the link at different load resistance at 13.56 MHz operating frequency and 10 mm transmission distance

Table 3: Optimized PSCs geometries and link parameters from simulation results*

Parameters	TX	RX
d_o (mm)	32	10
d_i (mm)	6.1	5
n (turns)	16	8
w (mm)	0.55	0.16
s (mm)	0.25	0.15
L (µH)	5.05	0.676
R_s (Ω)	3.07	1.12
C_p (pF)	2.27	1.05
C_1/C_2(pF)	25	203
Q	128	51
SRF (MHz)	47	189
k_{cal}♦	0.0797	
k_{sim}•	0.0803	
$\eta_{link\ cal}$♦	74.42%	
$\eta_{link\ sim}$•	73.46%	

*For face to face PSCs with a transmission distance of 10 mm at 13.56 MHz and 500 Ω load.
•Simulation results,
♦Calculation results.

Conclusion

Optimal printed spiral coil pair used in wireless power transfer system for implanted bio-medical devices is presented in this paper. We have devised a simple design procedure for optimizing the gross geometry of printed spiral coils to achieve maximum power transmission efficiency. Numerical calculation results and HFSS electromagnetic simulation denote that the power transmission efficiency of WPT link in air medium are in agreement and exceed 73%, which validates the concept of the physical models. Future work will cover, the modification of an optimization design algorithm for PSCs in tissues medium.

Comparison with Previously Published Works

Our work is compared to similar endeavors undertaken in this field, as summarized in Table IV. It can be observed that the power transfer efficiency achieved in this work is the highest with respect to coils distance and implant coil size.

Table 4: Comparison with previously published results

References	Year	Technique	Coil Shape	Operation Frequency	TX size (mm)		RX size (mm)		Efficiency (%) at 10 mm distance		Medium
					d_o	d_i	d_o	d_i	Calculation	Simulation	
U. Jow and M. Ghovanloo, 2008	2008	2coil	Square PSC	13.56 MHz	79	11.2	10	2.96	56.6	≈52*	Air
U. Jow and M. Ghovanloo, 2009	2009	2coil	Square PSC	13.56 MHz	38	14.9	10	5.8	72.05	74.86	Air
		2coil	Square PSC	13.56 MHz	30	11.1	10	5.5	55.22	49.12	Saline
		2coil	Square PSC	13.56 MHz	24	9.4	10	7.2	29.85	27.70	Muscle
W. Wu and Q. Fang, 2011	2011	2coil	Square PSC	13.56 MHz	28	8	10	6	77.5	71.1	Air
				8 MHz (shift)					-	15.2	Skin+ Fat
S. Stocklin, T. Volk, A. Yousaf, J. Albesa & L. Reindl, 2015	2015	2coil	Circular PSC	13.56 MHz	30	-	10	4.3	-	≈55*	Air
			Circular PSC with ferrite							≈60	
This work	2017	2coil	Square PSC	13.56 MHz	32	6.1	10	5	74.42	73.46	Air

References

P. Meyer, P. Germano, M. Markovic, and Y. Perriard (Jul./Aug. 2011.), Design of a Contactless Energy-Transfer System for Desktop Peripherals, IEEE Transactions on Industry Applications, vol. 47, no. 4, pp. 1643-1651

E. Waffenschmidt (Oct. 2011), Wireless power for mobile devices, IEEE International Telecommunications Energy Conference, Amsterda.

H. Marques and B. Borges (Oct. 2011), Contactless battery charger with high relative separation distance and improved efficiency, International Telecommunications Energy Conference.

U. Jow and M. Ghovanloo (Sep. 2007), Design and optimization of printed spiral coils for efficient transcutaneous inductive power transmission, IEEE Transactions on biomedical circuits and systems, vol. 1, no. 3, pp. 193–202.

U. Jow and M. Ghovanloo (Oct. 2009), Modeling and optimization of printed spiral coils in air, saline, and muscle tissue environments, IEEE transactions on biomedical circuits and systems, vol. 3, no. 5, pp. 339-347.

W. Wu and Q. Fang (2011), Design and simulation of printed spiral coil used in wireless power transmission systems for implant medical devices, Engineering in Medicine and Biology Society, EMBC, 2011 Annual International Conference of the IEEE, pp. 4018-4021.

S. Mutashar, M. A. Hannan, S. A. Samad, and A. Hussain, Analysis and optimization of spiral circular inductive coupling link for bio-implanted applications on air and within human tissue, Sensors, vol. 14. no. 7, pp. 11522-11541, 2014.

S. Stocklin, T. Volk, A. Yousaf, J. Albesa and L. Reindl (2015), Efficient Inductive Powering of Brain Implanted Sensors, Sensors Applications Symposium (SAS), 2015 IEEE. IEEE

S. Mehri, A. C. Ammari, J. Ben, H. Slama, and H. Rmili (June 2016), Geometry optimization approaches of inductively coupled printed spiral coils for remote powering of implantable biomedical sensors, in Proceedings of the Global Summit on Computer and Information Technology (GSCIT '14), pp. 1–11, Sousse, Tunisia.

C. Yang, C. Chang, S. Lee, S. Chang, and L. Chiou(2017), Efficient Four Coil Wireless Power Transfer for Deep Brain Stimulation, IEEE Transactions on Microwave Theory and Techniques, pp. 1-12.

G. M. Clark (2003), Cochlear implants, fundamentals and applications, AIP series in modern acoustics and signal processing by Beyer RT (editor in chief) Springer, New York.

M. S. Humayun, J. D. Weiland, G. Y. Fujii, R. Greenberg, R. Williamson, J. Little, B. Mech, V. Cimmarusti, G. V. Boemel , G. Dagnelie, and E. de Juan Jr. (Nov. 2003), Visual perception in a blind subject with a chronic microelectronic retinal prosthesis, Vision research, vol. 43, no. 24, pp. 2573–2581.

L. Chen, S. Liu, Y. C. Zhou, and T. J. Cui (2013.), An optimizable circuit structure for high-efficiency wireless power transfer, IEEE Transactions on Industrial Electronics, vol. 60, no. 1, pp. 339-349

G. Lazzi, Thermal effects of bioimplants (2005), IEEE Engineering in Medicine and Biology Magazine, vol. 24, no. 5, pp. 75–81.

P. Vaillancourt, A. Djemouai, J. F. Harvey and M. Sawan (Oct. 1997), EM radiation behavior upon biological tissues in a radio-frequency power transfer link for a cortical visual implant, Proceedings of 19th Annual International Conference of the IEEE, vol. 6, pp. 2499-2502.

K. Finkenzeller (2010), RFID handbook: fundamentals and applications in contactless smart cards, radio frequency identification and near-field communication. John Wiley & Sons.

S. S. Mohan, M. del Mar Hershenson, S. P. Boyd, and T. H. Lee (Oct. 1999), Simple accurate expressions for planar spiral inductances, IEEE Journal of Solid-State Circuits, vol. 34, no. 10, pp. 1419–1424.

S. Raju, R. Wu, M. Chan, and C. P. Yue (Jan. 2014.), Modeling of mutual coupling between planar inductors in wireless power applications, IEEE Transaction on Power Electronics, vol. 29, no. 1, pp. 481-490

S. Raju, C. C. Parawoto, M. Chan, and C. P. Yue (2015), Modeling of on-chip wireless power transmission system, Wireless Symposium (IWS), 2015 IEEE International. IEEE.

R. R. Harrison (2007), Designing efficient inductive power links for implantable devices, Circuits and Systems, 2007. ISCAS 2007. IEEE International Symposium on. IEEE.

S. M. Abbas, M. A. Hannan, and A. S. Salina (2012), Efficient class-E design for inductive powering wireless biotelemetry applications, Biomedical Engineering (ICoBE), 2012 International Conference on. IEEE.

Z. Yang, W. Liu, and E. Basham (Oct. 2007), Inductor modeling in wireless links for implantable electronics, IEEE Transactions on Magnetics, vol. 43, no. 10, pp. 3851–3860.